

High efficiency GeTe-based materials and modules for thermoelectric power generation

Xing Tong,^{a†} Qingfeng Song,^{a†} Pengfei Qiu,^{*ab} Qihao Zhang,^a Ming Gu,^a Xugui Xia,^a Jincheng Liao,^a Xun Shi^{*a} and Lidong Chen^{ac}

^aState Key Laboratory of High Performance Ceramics and Superfine Microstructure, Shanghai Institute of Ceramics, Chinese Academy of Sciences, Shanghai 200050, China.

^bSchool of Chemistry and Materials Science, Hangzhou Institute for Advanced Study, University of Chinese Academy of Sciences, Hangzhou 310024, China

^cCenter of Materials Science and Optoelectronics Engineering, University of Chinese Academy of Sciences, Beijing 100049, China

[†]Equally contributed to this work

Corresponding author: qiupf@mail.sic.ac.cn; xshi@mail.sic.ac.cn

Supplementary Information

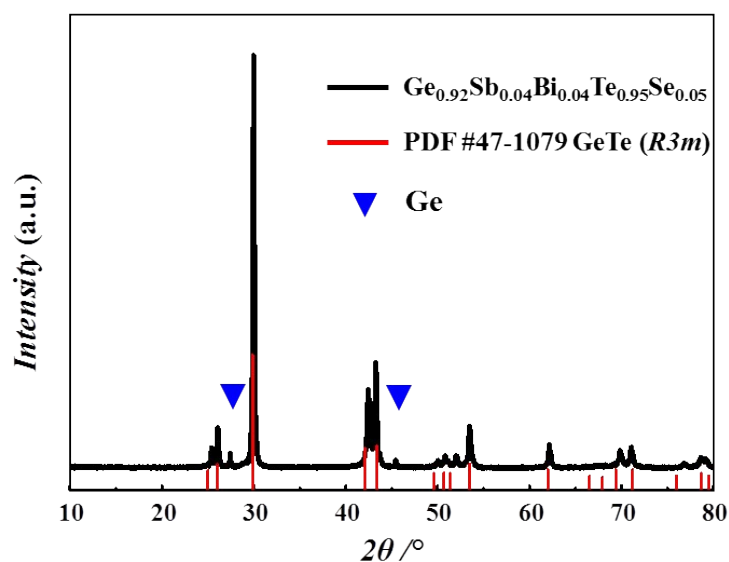


Fig. S1 Room temperature powder X-ray diffraction (XRD) pattern for



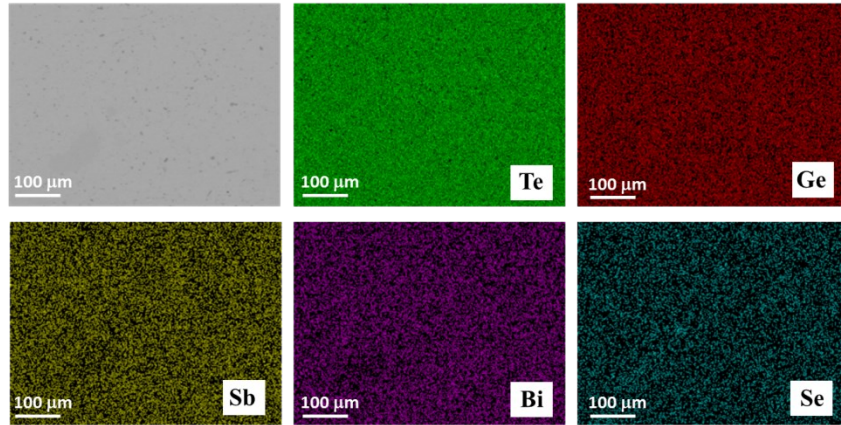


Fig. S2 Scanning electron microscopy (SEM) and energy dispersive spectroscopy (EDS) analyses for $\text{Ge}_{0.92}\text{Sb}_{0.04}\text{Bi}_{0.04}\text{Te}_{0.95}\text{Se}_{0.05}$.

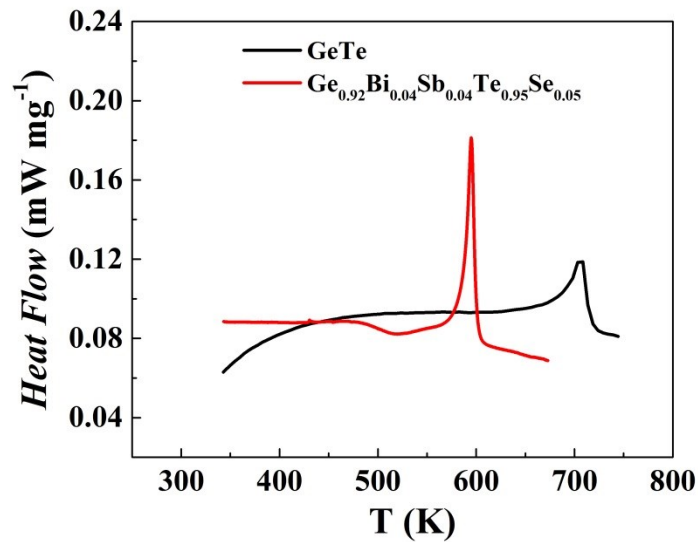


Fig. S3 Heat flow curves of GeTe and $\text{Ge}_{0.92}\text{Sb}_{0.04}\text{Bi}_{0.04}\text{Te}_{0.95}\text{Se}_{0.05}$ characterized by the differential scanning calorimetric (DSC) measurement.

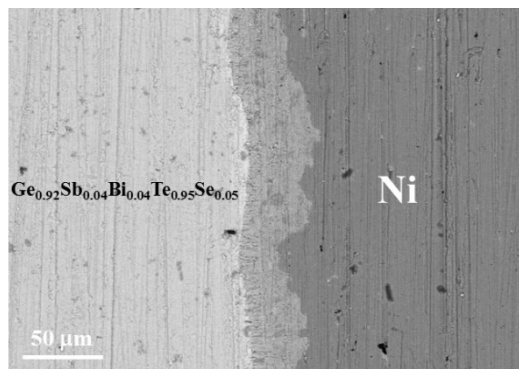


Fig. S4 Microstructure of the $\text{Ge}_{0.92}\text{Sb}_{0.04}\text{Bi}_{0.04}\text{Te}_{0.95}\text{Se}_{0.05}/\text{Ni}$ interface.

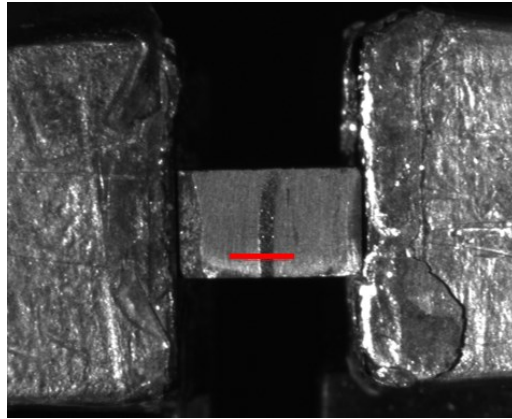


Fig. S5 GeTe/Mo/GeTe sandwich bar used for contact resistance measurement. The red line represents the moving track of probe.

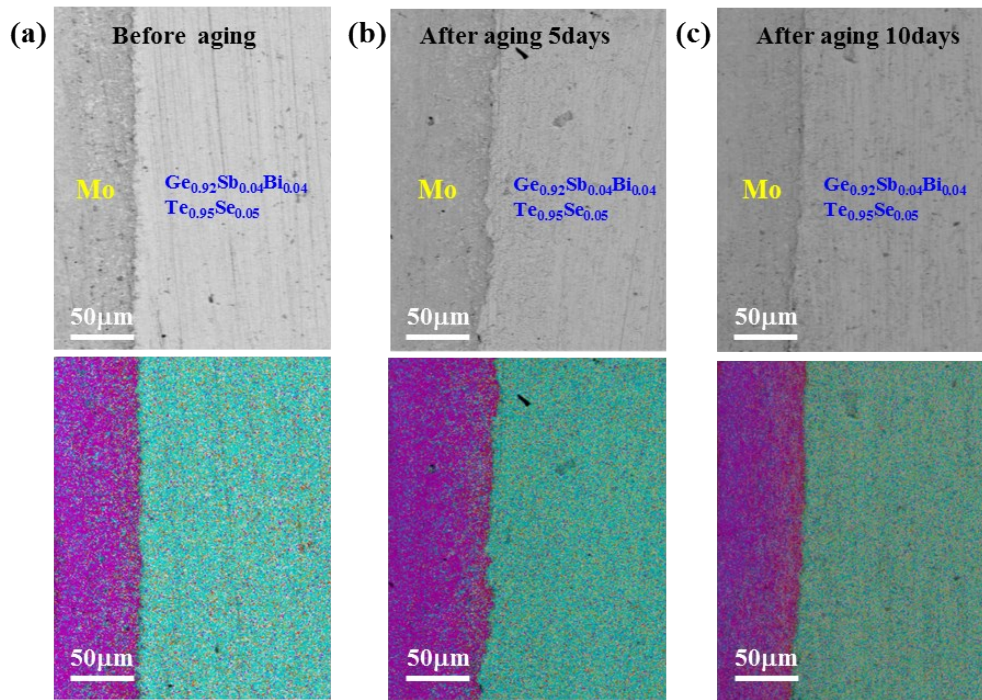


Fig. S6 Scanning electron microscopy and EDS elemental mapping performed on the interface area of the aged $\text{Ge}_{0.92}\text{Sb}_{0.04}\text{Bi}_{0.04}\text{Te}_{0.95}\text{Se}_{0.05}/\text{Mo}/\text{Ni}$ TE legs, (a) Before aging, (b) After aging 5 days, (c) After aging 10 days at 800 K.

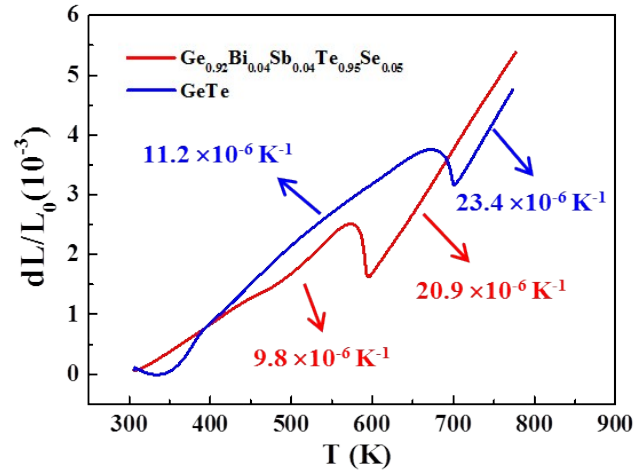


Fig. S7 Temperature dependence of relative length variation (dL/L_0) for GeTe and $\text{Ge}_{0.92}\text{Sb}_{0.04}\text{Bi}_{0.04}\text{Te}_{0.95}\text{Se}_{0.05}$. The values on the dL/L_0 curves represent the linear coefficient of thermal expansion (CTE) in the specific temperature range.



Fig. S8 Microstructure of the $\text{Ge}_{0.92}\text{Sb}_{0.04}\text{Bi}_{0.04}\text{Te}_{0.95}\text{Se}_{0.05}/\text{Mo}/\text{Ni}$ interface.

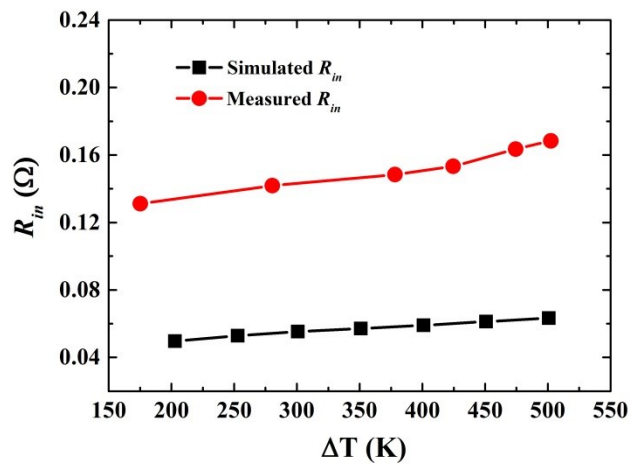


Fig. S9 Measured and simulated internal resistance R_{in} of $\text{Ge}_{0.92}\text{Sb}_{0.04}\text{Bi}_{0.04}\text{Te}_{0.95}\text{Se}_{0.05}/\text{Yb}_{0.3}\text{Co}_4\text{Sb}_{12}$ TE module

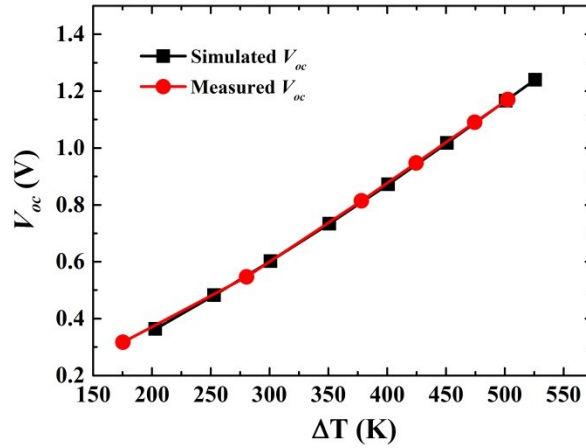


Fig. S10 Measured and simulated open voltage V_{oc} of $\text{Ge}_{0.92}\text{Sb}_{0.04}\text{Bi}_{0.04}\text{Te}_{0.95}\text{Se}_{0.05}/\text{Yb}_{0.3}\text{Co}_4\text{Sb}_{12}$ TE module

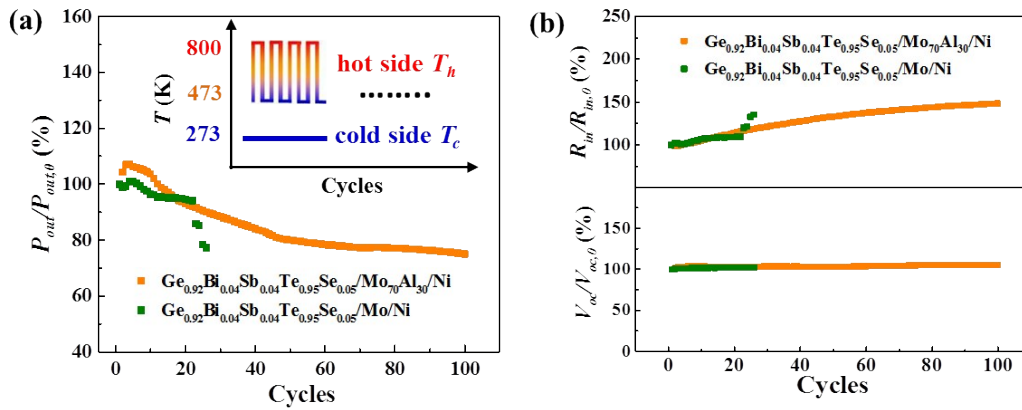


Fig. S11 Variations of (a) relative power output ($P_{out}/P_{out,0}$), (b) relative internal resistance ($R_{in}/R_{in,0}$) and relative open circuit voltage ($V_{oc}/V_{oc,0}$) for the $\text{Ge}_{0.92}\text{Sb}_{0.04}\text{Bi}_{0.04}\text{Te}_{0.95}\text{Se}_{0.05}/\text{Mo}/\text{Ni}$ and $\text{Ge}_{0.92}\text{Sb}_{0.04}\text{Bi}_{0.04}\text{Te}_{0.95}\text{Se}_{0.05}/\text{Mo}_{70}\text{Al}_{30}/\text{Ni}$ TE legs during thermal cycling test, where $P_{out,0}$, $R_{in,0}$ and $V_{oc,0}$ are the initial power output, initial internal resistance and initial open circuit voltage, respectively. The inset shows the schematic map of thermal cycling test. The hot side temperature is cycled from 473 K to 800 K. The cold side temperature is fixed at 300 K. The data are collected when the hot side temperature of the TE leg is 800 K.

Table S1 Thickness of reaction layers between GeTe and different pure metals. ‘N’ represents no diffusion layer is formed, and ‘C’ represents the barrier material reacted with GeTe completely.

| | Pure metals | Thickness (μm) |
|--------------------|-------------|-----------------------------|
| Category 1# | Ta | N |
| | Nb | N |
| Category 2# | Fe | C |
| | Ni | C |
| Category 3# | Mo | < 1 |
| | Ti | ~3 |
| | Hf | ~3 |
| | Cr | ~5 |
| | Zr | ~5 |
| | V | ~10 |
| | Co | ~20 |
| | Al | ~20 |

Table S2 The preset parameters used in the three-dimensional numerical analysis.

| | |
|---|--|
| Electrical contact resistance | 40 $\mu\Omega \text{ cm}^2$ |
| Thermal contact resistance of cold side | 1.2 $\times 10^4 \text{ Wm}^{-2}\text{K}^{-1}$ |
| Thermal contact resistance of hot side | 6 $\times 10^4 \text{ Wm}^{-2}\text{K}^{-1}$ |
| Thickness of filled glass fibers | 1 mm |
| Thermal conductivity of glass fibers | 0.9 $\text{Wm}^{-1}\text{K}^{-1}$ |
| Temperature of hot side | 800 K |
| Temperature of cold side | 300 K |